

# Influence of Fluorine Doping on Hardness and Compressive Stress of the Diamond-Like Carbon Thin Film

Sayed Mohammad Adel Aghili<sup>1</sup>, Raheleh Memarzadeh<sup>1†</sup>, Reza Bazargan Lari<sup>1†</sup>, and Akbar Eshaghi<sup>2</sup>

<sup>1</sup>Department of Materials Science and Engineering, Marvdasht Branch, Islamic Azad University, Marvdasht 73711-13119, Iran

<sup>2</sup>Department of Materials Engineering, Malek Ashtar University of Technology, Isfahan 83157-13115, Iran

(Received January 25, 2023 : Revised March 15, 2023 : Accepted March 22, 2023)

**Abstract** This study assessed the influences of fluorine introduced into DLC films on the structural and mechanical properties of the sample. In addition, the effects of the fluorine incorporation on the compressive stress in DLC films were investigated. For this purpose, fluorinated diamond-like carbon (F-DLC) films were deposited on cobalt-chromium-molybdenum substrates using radio-frequency plasma-enhanced chemical vapor. The coatings were examined by Raman scattering (RS), Attenuated total reflectance Fourier transform infrared spectroscopic analysis (ATR-FTIR), and a combination of elastic recoil detection analysis and Rutherford backscattering (ERDA-RBS). Nano-indentation tests were performed to measure hardness. Also, the residual stress of the films was calculated by the Stony equation. The ATR-FTIR analysis revealed that F was present in the amorphous matrix mainly as C-F and C-F<sub>2</sub> groups. Based on Raman spectroscopy results, it was determined that F made the DLC films more graphitic. Additionally, it was shown that adding F into the DLC coating resulted in weaker mechanical properties and the F-DLC coating exhibited lower stress than DLC films. These effects were attributed to the replacement of strong C=C by feeble C-F bonds in the F-DLC films. F-doping decreased the hardness of the DLC from 11.5 to 8.8 GPa. In addition, with F addition, the compressive stress of the DLC sample decreased from 1 to 0.7 GPa.

**Key words** fluorine doping, diamond-like carbon, hardness, compressive stress.

## 1. Introduction

DLC coatings have collected a considerable amount of devotion owing to their definite properties such as good chemical inertness, low friction, wear resistance, high hardness, water-resistance, low energy of the surface, temperature battle, anti-adherence of the bacteria, and biocompatibility and water-resistance ability.<sup>1-3)</sup> The combination of good mechanical properties, high abrasion resistor, chemical lifelessness, and biocompatibility makes DLC coating suitable for usage in the biomedical industry.<sup>2,4-6)</sup> However, because of the great compressive tension caused by ion bombardment during the deposition process, DLC films often have deprived bonds on some applied substrate, especially biomedical alloys, such as CoCrMo.<sup>7,8)</sup> To overawed of these restrictions,

other elements, for instance, Si, F, O, N, have been familiarized into DLC coatings.<sup>3,4,8-10)</sup>

Fluorine (F) is one of the greatest incapacitating DLC films to improve abrasion resistance, and water resistance.<sup>10-14)</sup> Moreover, there are different reports on the increase of inadaptability and reduction of bacterial adhesion of F-DLC sample in comparison to those of uncoated 316 L stainless steel and CoCrMo alloys.<sup>6,15)</sup> Dawei-Ren<sup>16)</sup> reported a reduction of bacterial adhesion by 60 % in F-doped DLC coatings, associated to that of the bare 316 L rust proof steel. It was shown that F-DLC coatings are hydrophobic coatings with a water contact angle of over 90°. <sup>17)</sup> Saitoa et al.<sup>18)</sup> reported a 4-time increase in the values of contact angle with human blood in F-doped DLC films, compared to that of silicon as the substrate material. F-DLC coatings are fabricated by various

<sup>†</sup>Corresponding author

E-Mail : [rmemarzadeh79@gmail.com](mailto:rmemarzadeh79@gmail.com) (R. Memarzadeh, Islamic Azad Univ.)

[rbazarganlari@gmail.com](mailto:rbazarganlari@gmail.com) (R. Bazargan Lari, Islamic Azad Univ.)

© Materials Research Society of Korea, All rights reserved.

This is an Open-Access article distributed under the terms of the Creative Commons Attribution Non-Commercial License (<http://creativecommons.org/licenses/by-nc/3.0>) which permits unrestricted non-commercial use, distribution, and reproduction in any medium, provided the original work is properly cited.

deposition approaches for example fluorocarbons and hydrocarbons. Some of the various methods used for incorporating fluorine into DLC coatings include cathodic vacuum arc evaporation, sensitive magnetron sputter, and radio-frequency plasma-boosted CVD (RF-PECVD).

Over the past years, numerous studies have been performed to assess F-DLC properties.<sup>17-21)</sup> To the best of our knowledge, there is no report on the effect of the F-doping on the hardness and compressive stress of the DLC coatings.

## 2. Materials and Methods

Silicon (100) and CoCrMo alloy were used as substrates. The CoCrMo samples were prepared by polishing using a 1  $\mu\text{m}$  diamond powder. Then, the CoCrMo samples were cleaned with ethanol, before putting them into the vacuum chamber. As a final cleaning step and for the initiation of the substrate's surface, a plasma engraving was accomplished (Table 1). For the enhancement of the adhesion between F-DLC coating and CoCrMo samples, a thin TiN interlayer (200 nm) was coated. The films were covered on the substrate utilizing an RF-PECVD apparatus. A mixture of methane ( $\text{CH}_4$ , purity of 99.995 %), carbon tetrafluoride ( $\text{CF}_4$ , purity of 99.995 %), and argon (Ar, purity of 99.995 %) was performed with  $\text{CH}_4/\text{Ar}$  and  $\text{CF}_4/\text{CH}_4$  flow ratios of 9/1 and 1/9, respectively, for the deposition of DLC and F-DLC coating.

The hydrogen content of the DLC and F-DLC films was measured using ERDA (R.B.S RF, USA). The film composition was also measured by scattering of RBS analysis (R.B.S RF, USA). The chemical bonds of the films were identified by ATR-FTIR (Bruker, USA). Raman scattering (Almega, Sweden) was applied to analyze the atomic arrangement of the films. The hardness (H) and Young's modulus (E) of the coatings were also characterized by the nanoindentation technique, using CSM Instruments (USA). The remaining stress was evaluated by calculating the curvature radius of the substratum before and after the fabrication of film by the profilometer (RAGA, Iran).<sup>22)</sup>

**Table 1.** Plasma etching conditions.

Pressure (Pa)	Gas type	Power (W)	Gas flow rate (sccm)	Time (min)
40	Ar	150	90	15

## 3. Results and Discussions

The composition and the hydrogen content of the DLC and F-DLC films were analyzed using RBS and ERDA detectors. The carbon, hydrogen, and fluorine concentrations in the coatings are exhibited in Table 2. The RBS measurements confirmed the incorporation of F in F-DLC film with a concentration of 1.50 at%. Moreover, it can be seen that F-DLC coatings had an inferior hydrogen concentration than DLC coatings. This indicated that F atoms substituted H atoms that link to C atoms in DLC films to form  $\text{CF}_x$  ( $x < 3$ ) groups.<sup>23)</sup>

Fig. 1 illustrates the ATR-FTIR analysis of F-DLC coatings at  $625\sim 2,000\text{ cm}^{-1}$ , and Table 3 shows a summary of all absorption peaks between carbon and fluorine. As can be observed, the ATR-FTIR peaks consisted of two wide groups in regions of  $1,000\sim 1,401\text{ cm}^{-1}$  and  $1,400\sim 1,900\text{ cm}^{-1}$  matching to  $\text{CF}_{x(x=1-3)}$  functional groups and  $\text{C}=\text{C}$  vibration modes, respectively.<sup>24-26)</sup> According to Huang et al.,<sup>25)</sup> the peak (with low intensity) at  $635\text{ cm}^{-1}$  can be attributed to the  $\text{CF}_2$  wagging mode. In addition, the band at  $730\sim 745\text{ cm}^{-1}$  is assigned to  $\text{CF}\text{-CF}_3$  bands.<sup>25)</sup> Two intense absorption bands detected at  $1,030$  and  $1,070\text{ cm}^{-1}$  were a result of  $\text{C}\text{-F}$  bonds, the high intensity of which can imply that there was plenty of  $\text{C}\text{-F}$  functional group in the F-DLC film. Moreover, low intense peaks at  $1,160$ ,  $1,220$ , and  $1,450\text{ cm}^{-1}$  are attributed to  $\text{CF}_2$  symmetric stretch modes.<sup>25-27)</sup> In DLC films where C is backbonded to H, the  $\text{C}=\text{C}$  functional group is usually detected at  $1,600\text{ cm}^{-1}$ ; however, according to the results of the ERDA test (Table 2) in F-DLC films in which the H atoms are substituted by F atoms, the  $\text{C}=\text{C}$  stretch shifts to higher frequency; accordingly,  $\text{C}=\text{CF}$  stretch modes are observed at the region of  $1,608\sim 1,700\text{ cm}^{-1}$ .<sup>28)</sup>  $\text{C}=\text{C}$  stretching and  $\text{F}_2\text{C}=\text{C}$  were perceived at  $1,700$  and  $1,720\text{ cm}^{-1}$ , separately. Additionally, the tiny absorbed peak at  $2,960\text{ cm}^{-1}$  was attributed to  $\text{sp}^3\text{ CH}_3$  bonds. These results confirm the corporation of F in F-DLC coatings. Furthermore, it was shown that F in F-DLC films was presented mainly in the form of  $\text{C}\text{-F}_{x(x=1,2)}$

**Table 2.** The carbon, hydrogen, and fluorine concentrations in DLC and F-DLC films.

Sample	C at%	F at%	H at%
DLC	74	-	26
F-DLC	74.5	1.5	24

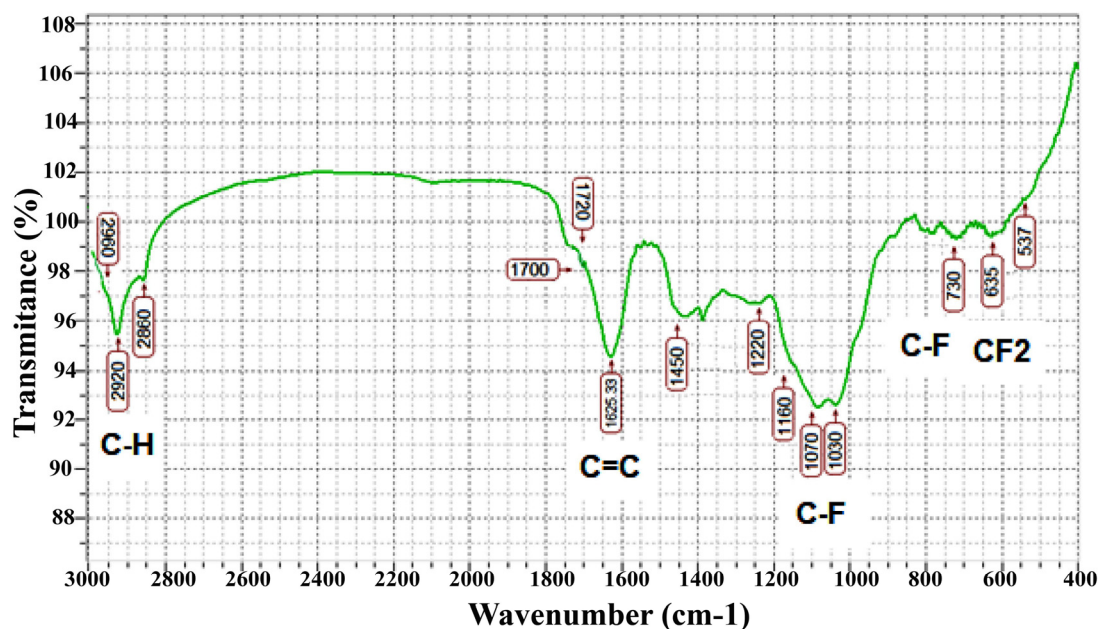


Fig. 1. ATR-FTIR spectroscopy of the F-DLC film.

Table 3. ATR-FTIR absorption spectra of F-DLC film<sup>25-28</sup>.

Chemical bond	Wavenumber (cm <sup>-1</sup> )	Functional group	Wavenumber (cm <sup>-1</sup> )
CF <sub>2</sub> symmetric stretching modes	1,450	CF <sub>2</sub> bending mode	537
C = C	1,608~1,700	CF <sub>2</sub> wagging mode	635
C = C stretching	1,700	CF-CF <sub>3</sub>	730~745
F <sub>2</sub> C = C	1,720	CF	1,030
sp <sup>3</sup> C-H <sub>2</sub>	2,860	CF	1,070
sp <sup>3</sup> CH, CH <sub>2</sub>	2,920	CF <sub>2</sub> symmetric stretch modes	1,160
sp <sup>3</sup> CH <sub>3</sub>	2,960	CF <sub>2</sub> symmetric stretch modes	1,220

groups which could significantly change the properties of F-DLC films, compared to those of DLC films.

Fig. 2 displays the Raman spectra of the films. The spectra of the coatings were split into D and G bands using two Gaussian diagrams. Then, for the structural characterization of the films and estimation of sp<sup>2</sup> content, the peak position, the G peak at FWHM, and the greatness of the D and G bands (I<sub>D</sub>/I<sub>G</sub> ratio) were obtained. Table 4 tabulates a summary of the chief features of the Raman scattering of DLC and F-DLC films. According to Table 4, the I<sub>D</sub>/I<sub>G</sub> ratio for F-DLC was upper than for DLC coatings. Considering that the G peak is a result of the stretching mode of sp<sup>2</sup> locations, although the D band was related to the breathing manner of the sp<sup>2</sup> site only in rings, not in chains, the higher I<sub>D</sub>/I<sub>G</sub> in F-DLC film implied that the concentration of sp<sup>2</sup> ring structure increased in the F-DLC films, compared to that of DLC films.<sup>29</sup> In

other words, the I<sub>D</sub>/I<sub>G</sub> ratio showed the opposite performance with the sp<sup>3</sup>/sp<sup>2</sup> hybrid ratio.

Therefore, a rise in the I<sub>D</sub>/I<sub>G</sub> ratio in F-DLC films can be recognized by the improved number of sp<sup>2</sup> hybridization and the construction of sp<sup>2</sup> of carbon areas.<sup>30-34</sup> Moreover, as can be observed in Table 4, the corporation of fluorine in DLC coatings led to the reduction of G-peak width in F-DLC films. G-peak width is a key factor to determine the relative concentration and the size of sp<sup>2</sup> clusters and structural order in films; accordingly, the lower G-peak width can be related to the higher concentration of sp<sup>2</sup> clusters and higher structural order in the film. Therefore, the results demonstrated a higher concentration of sp<sup>2</sup> bonding and more graphitic structure in the F-DLC films, which could lead to lower intrinsic stress in these films, associated with those of the DLC coatings.

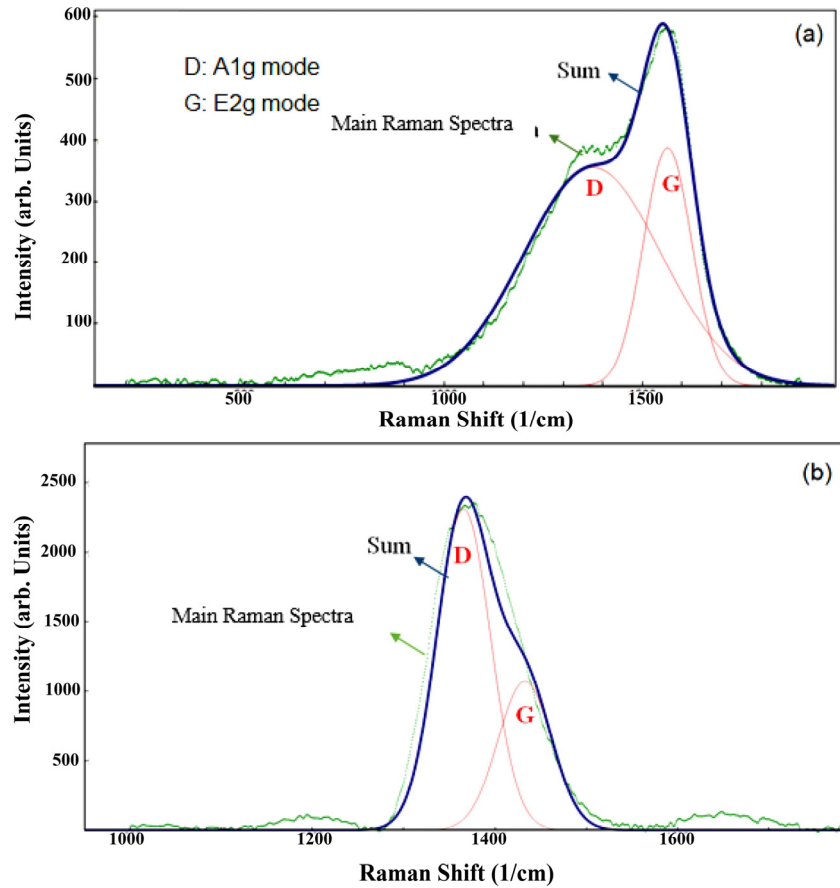


Fig. 2. Raman spectra of (a) DLC and (b) F-DLC films.

**Table 4.** The results of Raman spectroscopy of DLC and F-DLC films.

Sample	G peak position (cm <sup>-1</sup> )	D peak position (cm <sup>-1</sup> )	ID/IG	FWHM (G) (cm <sup>-1</sup> )
DLC	1,563.40	1,374.42	0.92	71.27
F-DLC	1,432.55	1,365.44	2.15	34.58

For the assessment of the inspiration of the F corporation on the mechanical features and compressive stress in the DLC films, hardness, Young's modulus, and the amounts of internal stress of both F-DLC and DLC films were evaluated. Table 5 shows the obtained results in this regard. It can be observed that F-DLC had a lower hardness and elasticity, compared to DLC film. Moreover, it can be seen that the addition of fluorine resulted in lower compressive stress in F-DLC films.

The mechanical properties are in a straight line proportionate to the C-C sp<sup>3</sup> portions in the microstructure of DLC coating; accordingly, the reduction of the C-C fraction is the

**Table 5.** Mechanical properties of DLC and F-DLC films.

Sample	Hardness (GPa)	Young's modulus (GPa)	Compressive stress (GPa)
DLC	11.50	109.00	1
F-DLC	8.80	97.00	0.7

main reason for the decline in mechanical properties.<sup>31-33)</sup> According to the Raman spectroscopy results the introduction of the F produced the alteration of sp<sup>3</sup> cross-connected nets into sp<sup>2</sup> carbon fields in DLC coatings. Thus, according to the F-DLC films, the drop in the rigidity and elastic modulus was attributed to the breaking of cross-linked C-C sp<sup>3</sup> bonds by the merger of the F atoms, which hints at a more open structural arrangement. Ma et al.<sup>35)</sup> also ascribed the reduction in mechanical properties of F-DLC films to the CF<sub>2</sub> quantity in the F-DLC coatings; accordingly, CF<sub>2</sub> groups can decrease the stiffness of the C-C network by breaching the carbon network.<sup>34,35)</sup> Some kind of literature<sup>36-58)</sup> also reported the reduction in the film mass with amassed doping concent-

ration as the reason for the sharp degradation in the mechanical properties and internal stress of F element doped-DLC coatings. In this study, the results of mechanical properties are in line with the outcomes of Raman scattering, indicating a decrease in the  $sp^3/sp^2$  ratio in F-DLC films. Regarding the compressive stress in F-DLC coatings, the lessening of interior stress with the amalgamation of F atoms was due to the reduction of the hydrogen content in F-DLC coatings. The presence of F atoms in DLC films caused the construction of HF unstable gas which decreases the content of hydrogen, particularly the unbound hydrogen.<sup>37-46</sup> Moreover, lower stress in the F-DLC coatings can be recognized as the decrease in the atomic density of the F-DLC coatings by replacing hydrogen with fluorine. It was stated that an inferior atomic mass and the revolution from a metastable  $sp^3$  to an unchanging  $sp^2$  conformation to some level can decrease the stiffness of the carbon net and lastly reasons for the fall of the internal stress.<sup>23)</sup>

#### 4. Conclusion

DLC and F-DLC coatings were covered on CoCrMo substrates by an rf-PECVD system with  $CH_4$  and  $CF_4 + CH_4$  gas combinations, respectively. A higher concentration of graphitic structure in F-DLC films was created which was confirmed by G-scattering mode in Raman analysis. Fluorine incorporation induced a decrease in the compressive stress (1 to 0.7 GPa), hardness (11.5 to 8.8 GPa), and elastic modulus (109 to 97 GPa) of the DLC films. Elastic recoil detection analysis and Rutherford backscattering (ERDA-RBS) results showed that doping with fluorine element reduces the amount of hydrogen in the structure from 26 % to 24 %. According to ATR-FTIR results, fluorine has replaced hydrogen in the structure. On the other hand, according to the results of Raman analysis, doping with fluorine causes a decrease in hybridization  $sp^3$  and an increase in hybridization  $sp^2$ . Therefore, the reduction of the atomic density and the reduction of the unstable phases  $sp^3$  happened, and therefore the hardness and compressive stress in the structure are reduced.

#### References

1. W. Liao, C. R. Lin, D. Wei, Y. R. Shen, Y. C. Li, J. A. Lee and C. Y. Liang, *J. Biomed. Mater. Res.*, **100**, 3151 (2012).

2. G. Dearnaley and J. H. Arps, *Surf. Coat. Technol.*, **200**, 2518 (2005).
3. J. Corona-Gomez, S. Shiri, M. Mohammadtaheri and Q. Yang, *Surf. Coat. Technol.*, **332**, 120 (2017).
4. D. K. Rajak, A. Kumar, A. Behera and P. L. Menezes, *Appl. Sci.*, **11**, 4445 (2021).
5. A. Muthuraja, S. Naik, D. K. Rajak and C. I. Pruncu, *Diamond Relat. Mater.*, **100**, 107588 (2019).
6. K. Yonezawa, M. Kawaguchi, A. Kaneuji, T. Ichiseki, Y. Inuma, K. Kawamura, K. Shintani, S. Oda, M. Taki and N. Kawahara, *J. Antibiot.*, **9**, 495 (2020).
7. P. Safaie, A. Eshaghi and S. R. Bakhshi, *Diamond Relat. Mater.*, **70**, 91 (2016).
8. P. Wang, X. Wang, T. Xu, W. Liu and J. Zhang, *Thin Solid Films*, **515**, 6899 (2007).
9. D. Koshel, H. Ji, B. Terreault, A. Cote, G. G. Ross, G. Abel and M. Bolduc, *Surf. Coat. Technol.*, **173**, 161 (2003).
10. M. Toyonaga, T. Hasebe, S. Maegawa, T. Matsumoto, A. Hotta and T. Suzuki, *Diamond Relat. Mater.*, **119**, 108558 (2021).
11. Z. Q. Yao, P. Yang, N. Huang, H. Sun and J. Wang, *Appl. Surf. Sci.*, **230**, 172 (2004).
12. F. R. Marciano, E. C. Almeida, D. A. Lima-Oliveira, E. J. Corat and V. J. Trava-Airoldi, *Diamond Relat. Mater.*, **19**, 537 (2010).
13. J. Wang, J. Ma, W. Huang, L. Wang, H. He and C. Liu, *Surf. Coat. Technol.*, **316**, 22 (2017).
14. T. Imai, T. Harigai, T. Tanimoto, R. Isono, Y. Iijima, Y. Suda, H. Takikawa, M. Kamiya, M. Taki and Y. Hasegawa, *Vacuum*, **167**, 536 (2019).
15. S. Onodera, S. Fujii, H. Moriguchi, M. Tsujioka and K. Hirakuri, *Diamond Relat. Mater.*, **107**, 107835 (2020).
16. D. Ren, Ph. D. Thesis (in English), p. 25-38, University of Dundee, Dundee, Scotland (2015).
17. M. Ishihara, T. Kosaka, T. Nakamura, K. Tsugawa, M. Hasegawa, F. Kokai and Y. Koga, *Diamond Relat. Mater.*, **15**, 1011 (2006).
18. T. Hasebe, S. Nagashima, A. Kamijo, T. Yoshimura, T. Ishimaru, Y. Yoshimoto, S. Yohena, H. Kodama, A. Hotta and K. Takahashi, *Thin Solid Films*, **516**, 299 (2007).
19. H. Schulz, M. Leonhardt, H. J. Scheibe and B. Schultrich, *Surf. Coat. Technol.*, **200**, 1123 (2005).
20. H. Ishige, S. Akaike, T. Hayakawa, M. Hiratsuka and Y. Nakamura, *Dent. Mater. J.*, **38**, 424 (2019).
21. L. Liu, W. Tang, Q. Ruan, Z. Wu, C. Yang, S. Cui, Z. Ma, R. Fu, X. Tian and R. Wang, *Surf. Coat. Technol.*, **404**, 126468 (2020).
22. P. J. Martin, A. Bendavid, M. Swain, R. P. Netterfield, T. J. Kinder, W. G. Sainty, D. Drage and L. Wielunski, *Thin*

- Solid Films, **239**, 181 (1994).
23. L. Zhang, F. Wang, L. Qiang, K. Gao, B. Zhang and J. Zhang, *RSC Adv.*, **5**, 9635 (2015).
  24. G. D. Fu, E. T. Kang and K. G. Neoh, *J. Phys. Chem.*, **107**, 13902 (2003).
  25. K. P. Huang, P. Lin and H. C. Shih, *J. Appl. Phys.*, **96**, 354 (2004).
  26. N. M. Mackie, D. G. Castner and E. R. Fisher, *Langmuir*, **14**, 1227 (1998).
  27. G. Chen, J. Zhang and S. Yang, *Electrochem. Commun.*, **10**, 7 (2008).
  28. D. C. Marra and E. S. Aydil, *J. Vac. Sci. Technol., A*, **15**, 2508 (1997).
  29. A. C. Ferrari and J. Robertson, *Philos. Trans. R. Soc., A*, **362**, 2477 (2004).
  30. A. C. Ferrari and J. Robertson, *J. Phys.*, **61**, 14095 (2000).
  31. J. Robertson, *Phys. Rev. Lett.*, **68**, 220 (1992).
  32. A. C. Ferrari, J. Robertson, M. G. Beghi, C. E. Bottani, R. Ferulano and R. Pastorelli, *Appl. Phys. Lett.*, **75**, 1893 (1999).
  33. M. Samadi, A. Eshaghi, S. R. Bakhshi and A. A. Aghaei, *Opt. Quantum Electron.*, **50**, 1 (2018).
  34. F. L. Freire Jr, M. Costa, L. G. Jacobsohn and D. F. Franceschini, *Diamond Relat. Mater.*, **10**, 125 (2001).
  35. X. Ma, G. Tang and M. Sun, *Surf. Coat. Technol.*, **201**, 7641 (2007).
  36. L. G. Jacobsohn, M. Costa, V. J. Trava-Airoldi and F. L. Freire, *Diamond Relat. Mater.*, **12**, 2037 (2003).
  37. A. Grill and D. Patel, *Diamond Relat. Mater.*, **2**, 1519 (1993).
  38. K. Q. Al-Hamad, M. Al-Omari, A. Al-Wahadni and A. Darwazeh, *J. Contemp. Dent. Pract.*, **7**, 29 (2006).
  39. K. Al Hamad, M. M. Qadan and A. M. Al Wahadni, *J. Esthetic Restor. Dent.*, **28**, S56 (2016).
  40. J. Müssig and N. Graupner, *A Critical Review. Rev. Adhes. Adhes.*, **8**, 68 (2021).
  41. P. Brown and P. Mazumder, *Rev. Adhes. Adhes.*, **9**, 123 (2021).
  42. C. Della Volpe and S. Siboni, *Rev. Adhes. Adhes.*, **10**, 47 (2022).
  43. M. Ghasemvand, B. Behjat and S. E. Ebrahimi, *J. Adhes.*, **98**, 1 (2022).
  44. A. K. Netam, V. P. Bhargava, R. Singh and P. Sharma, *J. Complementary Med. Res.*, **12**, 204 (2021).
  45. S. D. Wani and A. Mundada, *Int. J. Pharm. Res. Technol.*, **11**, 1 (2021).
  46. M. S. Sabzi, H. M. Anijdan, M. Shamsodin, M. Farzam, A. Hojjati-Najafabadi, P. Feng, N. Park and U. Lee, *Coatings*, **13**, 188 (2023).

## Author Information

### Sayed Mohammad Adel Aghili

Ph. D. Student, Department of Materials Science and Engineering, Marvdasht Branch, Islamic Azad University

### Raheleh Memarzadeh

Assistant Professor, Department of Materials Science and Engineering, Marvdasht Branch, Islamic Azad University

### Reza Bazargan Lari

Assistant Professor, Department of Materials Science and Engineering, Marvdasht Branch, Islamic Azad University

### Akbar Eshaghi

Associate Professor, Department of Materials Engineering, Malek Ashtar University of Technology